11th Australasian Fluid Mechanics Conference
University of Tasmania, Hobart, Australia
14-18 December 1992

THE CHARACTER OF THE INSTABILITY OF THE SEPARATED SHEAR LAYER FROM A SQUARE LEADING EDGE FLAT PLATE

Julio SORIA and Jie WU

CSIRO Division of Building, Construction & Engineering
PO Box 56, Highett, VIC 3190, AUSTRALIA

ABSTRACT

The character of the unsteadiness of the shear layer separating from a square leading edge flat plate has been investigated using flow visualisation and hot-film spectral measurements. The Reynolds number for these experiments was 900 based on the thickness of the plate and the upstream mean velocity. A test plate with a chord to thickness ratio of 10 was used. The experiments were conducted in a closed circuit water tunnel with and without external perturbations. The perturbations were applied by oscillating the side walls of the water tunnel test section normal to the mean flow direction. The flow visualisations of the separated shear layer show the generation of a downstream growing vorticity wave. The analysis of velocity fluctuation spectra measured along the mean trajectory of the separated shear layer shows the existence of a frequency at which the velocity oscillations in the shear layer grow fastest in the downstream direction. This frequency is found to be approximately equal for both the unforced and forced case.

NOTATION

f	frequency
G_{uu}	auto-spectrum of u
G_{au}	cross-spectrum between signal a and u
h	plate thickness
Re	Reynolds number, hU_∞/ν
U_∞	mean upstream velocity
U	mean streamwise velocity
u	fluctuating streamwise velocity
x	streamwise coordinate along the midspan of the plate surface
y	coordinate normal to the plate surface
z	coordinate normal to the streamwise direction along the plate surface
α_i	spatial amplification rate
ν	kinematic viscosity

INTRODUCTION

The separated flow from a rectangular plate is a prototypic flow for many important engineering geometries. The many complex physical features of separated flows have been the subject of on-going research for a significant number of years. Kiya and Sasaki (1983), Cherry *et al.* (1984) and Sigurdson (1986) have studied the separation and re-attachment process. These studies have shown the highly unsteady nature of these flows, and that much of the flow is dominated by vortical structures.

The development of vortical structures in the separation bubble from bluff plates at moderate Reynolds numbers has been reported by flow visualisations of Lane and Loehrke (1980), Kiya (1986), Sigurdson (1986) and Soria *et al.* (1991). The development of three-dimensionalities in separated flows has also received recent attention. In particular, it has been observed (Kiya *et al.*, 1983, Sigurdson 1986 and Soria *et al.*, 1991) that cross-stream vorticity realigns into streamwise vorticity forming vortex loops which arrange into a staggered pattern.

The results presented here are a study of the vorticity waves which develop in the shear layer separating from the sharp leading edge of a rectangular plate. In particular, Soria *et al.* (1991) hypothesised that the development of the three-dimensional structures at moderate Reynolds numbers are dependent on the evolution characteristics of the separated shear layer, and further, that over much of its spatial development, the shear layer evolves in a similar way to a plane mixing layer. The shear layer grows primarily due to its instability characteristic, but as observed by Soria *et al.* (1991), shear layer growth is also due to pairing of vortical structures. In fact, the shear layer keeps on growing by pairing until it begins to be influenced by the plate. It is at this stage, that the vortical structure is observed to pinch off the separation bubble.

The aim of this investigation is to study the stability characteristics of the separated shear layer and to investigate if there exists a frequency, at which the velocity fluctuations in the shear layer grow spatially the fastest, i.e. is the shear layer instability convective? Both the natural disturbance environment of the water tunnel and forced perturbations are used in this study.

The cartesian coordinate system used to describe the geometry is such that the x-axis points along the plate surface in the streamwise direction. The y-axis points normal to the plate surface and the z-axis is normal to the main flow direction along the plate surface with $z = 0$ the midspan of the test plate. The origin of the coordinate system is positioned at the sharp separation edge of the rectangular plate.

EXPERIMENTAL APPARATUS AND TECHNIQUE

Water Tunnel Facility And Test Plate Details

The experiments were conducted in a closed circuit

water tunnel facility with a 244 mm square test section and a maximum test section velocity of 400 mm/s. Fig 1 shows a schematic of this water tunnel. The test section of this facility has flexible mounted side walls, which allow the imposition of synchronised wall oscillations perpendicular to the main flow direction. It is 770 mm long with the two 400 mm long movable side walls having glass windows. These two walls are rigidly connected to each other and are sealed to the remainder of the test section by a thin flexible membrane. The oscillations of the side walls are produced by an electromagnetic exciter fixed rigidly to the movable test section walls which is capable of 5 mm peak amplitudes. The harmonic distortions of the side wall oscillation are higher at the lower frequencies. Typically, in terms of wall velocity the 1st harmonic is -23 dB and the 2nd harmonic is -11 dB below the fundamental forcing frequency, higher harmonics are not observable. The oscillating test section wall displacements were monitored using a Schlumberger DG5 displacement transducer. In the present investigation random noise oscillations low-pass filtered at 10 Hz with a rms test section wall velocity of 0.007 % of U_∞ were used.

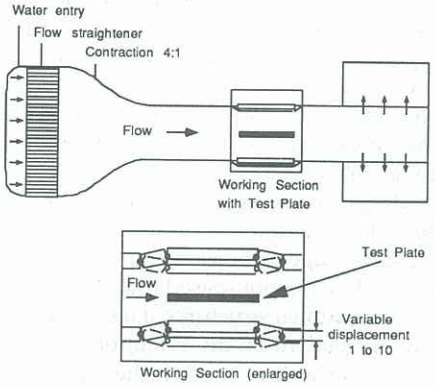

Fig 1 Schematic of water tunnel and test plate arrangement in the test section.

The mean flow velocity in the tunnel test section is generated by a pump driven by an AC electric motor which is accurately controlled by an electronic AC 3-phase motor controller. Hot-film traverses and particle image velocimetry (PIV) measurements have shown that the mean velocity variation across the test section is less than 1 %. For the mean velocities used in the present investigation, the mean turbulence level is approximately 0.09 % (low-pass filtered at 20 Hz), with the natural turbulence spectrum decaying at 200 dB/decade. No distinct spectral peaks are observable in the natural turbulence spectrum in the frequency range of interest. Further details of this water tunnel facility can be found Welsh *et al.* (1991).

Two geometrically identical rectangular test plates 13 mm thick, 130 mm chord and 244 mm span were used in these experiments. The plates were constructed from acrylic, machined flat and polished. One of the plates has a thin shim mounted flush on its upstream facing surface to generate hydrogen bubbles. This arrangement allows the release of a bubble sheet along most of the span of the plate. The other plate allows the injection of chloro-fluorescein dye through a 0.5 mm hole located on the midspan of its upstream facing surface. The fluorescent dye was injected at a low enough velocity so as not to disturb the boundary layer along the upstream facing surface of the rectangular plate. The particular test plate used was mounted vertically along the centerline of the test section without end plates. The Reynolds number based on the thickness of the plates (h) and the upstream mean free-stream velocity ($U_\infty = 70mm/s$) was 900 during this investigation.

Flow Visualisation

The flow visualisations were undertaken with hydrogen bubbles and chloro-fluorescein dye. A 4 W Argon-ion laser was used to visualise the hydrogen and the fluorescein dye. A high resolution Videk CCD camera with a 1280 x 1024 pixel array was used to capture the flow images. This camera has an intensity dynamic range of 48 dB. The exposure period of the CCD was controlled by modulating the laser with an acoustic optical modulator (AOM). Typical exposure periods ranged from 10 ms - 40 ms. Both the CCD camera and the AOM were controlled by a 386 PC using specific software written for image acquisition with this equipment. In order to extract fine features from the flow, the laser beam was fanned out into a thin laser sheet of approximately 1 - 2 mm thickness.

During all flow visualisations in the x-y plane, the laser sheet was located in the midspan of the test plate. A mean image was produced by asynchronously acquiring multiple images (typically, 50 - 100 images) and averaging the intensity at each pixel. The averaging was performed on the run. Phase-triggered averaging was also performed by acquiring individual images whenever the PC control program encountered a trigger level from a given AC signal (e.g. the displacement transducer signal monitoring the section wall oscillation). Further image enhancement of flow visualisation images was performed on Silicon Graphics (SGI) workstations.

Velocity Fluctuation Measurements and Data Analysis

The unsteady velocities in the free-stream and in the separated shear layer were measured using a TSI IFA 100 multi-channel constant temperature anemometer (CTA). TSI 1260A-10W miniature probes with $25\mu m$ diameter and $510\mu m$ long sensors were used for all measurements. The CTA system was calibrated before and after each measurement sequence using the three term CTA system equation (details can be found in Soria and Norton, 1990). Two hot-film sensors were used in the unforced experiments, one hot-film was positioned just upstream of the test plate and approximately 2-3 test plate thickness laterally displaced in the free-stream. This sensor was used to determine the "natural" disturbance environment. The other hot-film was used to measure the flow velocity along the mean separated shear layer trajectory. In the forced experiments the characteristics of the disturbance environment were determined from the velocity measurement of the oscillating test section walls.

Fig 2 shows the mean trajectory of the shear layer separating from the sharp leading edge of the rectangular plate (fluorescent dye, flow is left to right). The hot-film sensor was accurately positioned along this arc using real time images captured by the CCD camera and the image shown in Fig 2. At each measuring station, the position of the hot-film senor was accurately determined from the CCD image with a resolution of $100\mu m$.

The two hot-film (or hot-film/displacement trans-

ducer) analog signals were simultaneously digitised using a 12-bit A/D Boston board controlled by a 486 PC. Prior to digitising, the analog signals were low-pass filtered at 10 Hz, DC offset and suitably amplified to optimise the resolution over the $\pm 5V$ digitising range. A sampling frequency of 20 Hz was used for the acquisitions. The digitised time series were 4096 points long.

The entire post-processing of the data was performed on a SGI workstation. The CTA time series were digitally linearized by using the inverted function of the three term hot-film system equation (Soria and Norton, 1990) prior to any spectral analysis. Software to perform the averaged spectral analysis of the two channel data was developed. This program calculates the auto-spectral densities of both channels, in addition to the cross-spectral density, coherence function and other relevant spectral functions. The spectral analysis was performed on 512 point long time records, resulting in a spectral resolution of 0.04 Hz.

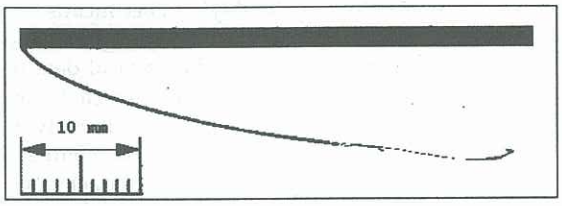

Fig 2 Mean trajectory of the separated shear layer from the sharp leading edge of the test plate.

RESULTS AND DISCUSSION

The fluorescent dye flow visualisation in Fig 3 (a) shows a streak line of the instantaneous separated shear layer in its unforced state (flow is left to right). Note the regular swellings in the dye, which become more pronounced in the downstream direction. Fig 3 (b) and (c) are the corresponding forced streak line flow visualisations (random test section wall velocity oscillations). The perturbations in the shear layer are considerably larger, even though the rms velocity oscillation over 0 - 10 Hz amounts to only 0.007 % of U_∞. Corresponding flow visualisations using hydrogen bubbles reveal details of the vortical nature of the shear layer showing the amplification process and the pairing process that these vortical structures undergo. Fig 3 (a) and (b) also show the hot-film probe in the image, indicating the relative dimensions of the phenomena under study and the sensor. There is no observable effect on the shear layer development from the hot-film probe.

The hot-film velocity oscillation measurements and analysis were undertaken on the following assumptions: (i) the instability in the shear layer is spatial in nature; (ii) the mean flow is parallel, i.e. the rate of change of U in x << the rate of change of U in y; (iii) the mean separated shear layer trajectory corresponds to the same spatial position in the disturbance eigenfunction profile for all points along this arc. Based on these assumptions, it can be shown that

$$\alpha_i = -\frac{\ln \frac{G_{uu}(x_1,f)}{G_{uu}(x_0,f)}}{2(x_1-x_0)} = -\frac{\ln \left| \frac{G_{uu}(x_1,f)G^*_{uu}(x_0,f)}{|G_{uu}(x_0,f)|^2} \right|}{(x_1-x_0)} \qquad (1)$$

$G_{uu}(x_i, f)$ is the auto-spectrum of u at x_i along the mean trajectory of the shear layer, while $G_{uu}(x_i, f)$ is the cross-spectrum between u and a - the oscillating wall velocity (or the natural free-stream velocity in the unforced case) . The * denotes the complex conjugate.

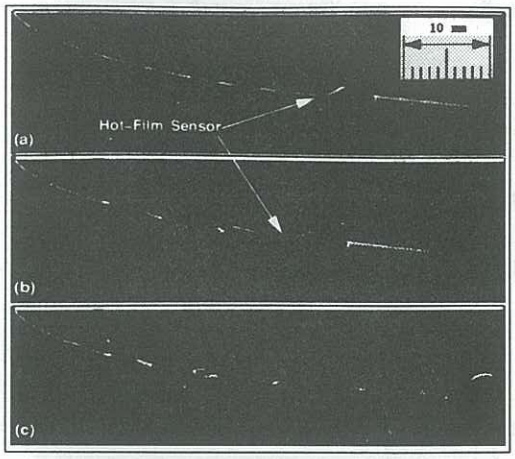

Fig 3 Instantaneous Flow Visualisation of the Separated Shear Layer. (a) Unforced, (b), (c) Forced.

Fig 4 shows the spatial evolution of the velocity spectrum along the shear layer (the solid line), the dashed line is the velocity spectrum in the free-stream and the dotted line is the transfer function between both these velocity oscillations in the flow. Consideration of any of Fig 4 (a) - (c) in isolation, results in the observation of the development of distinct spectral peaks. However, closer inspection of the these spectra together shows the fastest growing region in the spectrum to be between 2 - 2.5 Hz, with the auto-spectrum growing by as much as 3 orders of magnitude in this frequency range. Using 15 - 20 discrete measuring points along the shear layer, the amplification rate was estimated at each spectral line by applying a chi-least squared fit to a variation of eq (1). Two independent estimates for the amplification factor are possible, as shown in eq (1). Fig 5 shows the amplification factor as a function of frequency for the forced case. This result shows that indeed, the fastest growing modes of this shear layer for the given conditions have temporal frequencies between 2.2 - 2.5 Hz.

Naturally, there is a single frequency for the fastest growing mode, however, based on the limited measurements, only the general qualitative trend is given here. The ratio between the peak of the curve originating

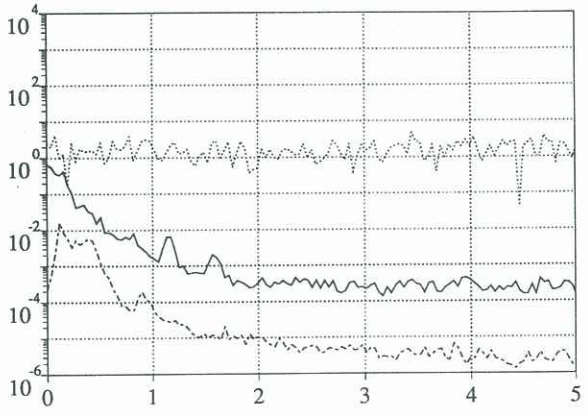

(a) $x/h = 0.8$

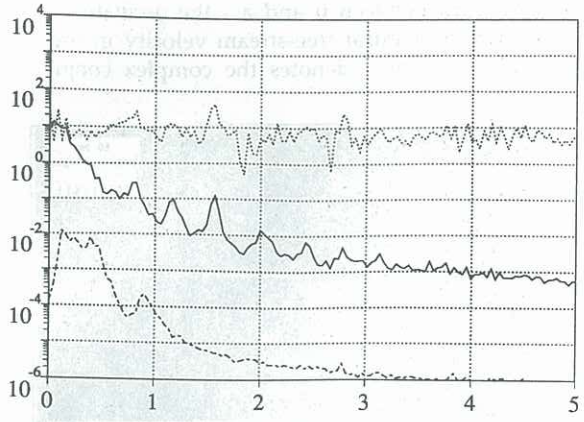

(b) $x/h = 2.6$

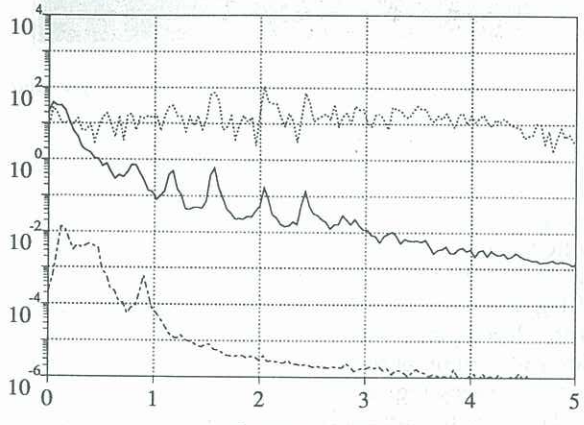

(c) $x/h = 4.0$

Fig 4 Downstream Development of Unforced Velocity Fluctuation Spectra Along Mean Separated Shear Layer Trajectory; solid line - G_{uu} shear layer, dashed line - G_{uu} free-stream, dotted line - transfer function.

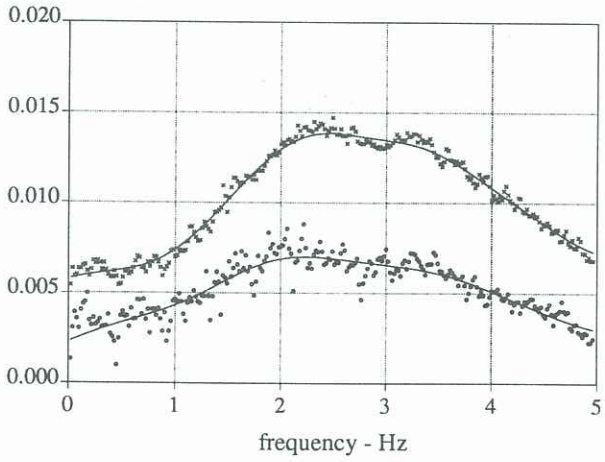

Fig 5 Spatial Amplification Rate α_i as a Function of Temporal Frequency. x - $2\alpha_i$, calculated using the auto-spectrum; o - α_i, calculated using the cross-spectrum; solid line - smoothed curves.

from the auto-spectra and the curve originating from the cross-spectra is approximately 2, as predicted by (1). The corresponding data for the natural case has a similar maximum hump between 2.2 - 2.5 Hz, but the scatter of this data is larger. The distribution of the spatial amplification factor with frequency compares qualitatively well with the spatial amplification characteristics for plane mixing layers (Michalke, 1965). Direct quantitative comparison for the present experimental geometry is complicated due to the small physical size of the shear layer and the nearly impossible task of determining momentum thickness and other relevant parameters. Nevertheless, the results presented here, show clearly that the instability of the separated shear layer is convective in nature, with a fastest growing spatial mode having a temporal frequency between 2.2 - 2.5 Hz.

CONCLUSIONS

The flow visualisations and spectral measurements of this investigation have shown that the separated shear layer from a rectangular flat plate has a spatial instability character (convective instability). This means that some velocity fluctuations in the shear layer grow exponentially in space. The analysis of the spectral data for unforced and small forcing has revealed the existence of a maximum spatial amplification rate at approximately the same temporal frequency. This characteristic compares favourably with the spatial amplification characteristics of plane mixing layers, in a qualitative sense. Other characteristics observed from flow visualisations also indicate that the character of the separated shear layer is very similar to that of plane mixing layer, i.e. the growing of the shear layer by the pairing process.

REFERENCES

CHERRY, N.L., HILLIER, R. and LAUGHTER, M.E.M.P. (1984) Unsteady Measurements in a Separated and Reattaching Flow. J Fluid Mech, 144, 13-46.

KIYA, M. and SASAKI, K. (1983) Structure of a Turbulent Separation Bubble. J Fluid Mech, 137, 83-113.

KIYA, M. (1986) Vortices and Unsteady Flow in Turbulent Separation Bubbles. Proc 9th Australasian Fluid Mech Conf, Auckland, 1-6.

LANE, J.C. and LOEHRKE, R.I. (1980) Leading Edge Separation From a Blunt Plate at Low Reynolds Number. ASME J Fluids Eng, 102, 494-496.

MICHALKE, A. (1965) On Spatially Growing Disturbances in an Inviscid Shear Layer. J Fluid Mech, 23, 521 - 544.

SIGURDSON, L.W. (1986) The Structure and Control of a Turbulent Reattaching Flow. PhD Thesis, California Institute of Technology.

SORIA, J.and NORTON, M.P. (1990) A Study of the Three Term Hot-Wire System Equation and Analog Linearization Based on It. Exp Thermal and Fluid Sci, 3, 346-353.

SORIA, J., SHERIDAN, M. and WELSH, M.C. (1991) Three-dimensionalities in Natural and Perturbed Separated Unsteady Flow From a Square Leading Edge Plate. Bull Am Phys Soc, 36,2691.

WELSH, M.C., HOURIGAN, K., WELCH, L.W., DOWNIE, R.J., THOMPSON, M.C. and STOKES, A.N. (1991) Acoustics and Experimental Methods: The Influence of Sound on Flow and Heat Transfer. Exp Thermal and Fluid Sci, 3, 138-152.